

# Simulation of Self Similar Random Processes and its Parameters Estimation

J. L. Hamkalo (1), J. M. Medina (1,2), A. Mailing (1), F. Dobarro (3), D. Fernandez (3,4), B. Cernuschi-Frías (1,2).

(1) Facultad de Ingeniería, Universidad de Buenos Aires (2) IAM-CONICET

(3) Universidad Nacional de Tierra del Fuego

(4) CADIC-CONICET

TE: +(11)4343-0891 int. 278, FAX: +(11)4331-1852

Email: jhamkal@fi.uba.ar

**Abstract.** An estimator of the self-similarity parameter for certain classes of random processes is presented. Simulation of synthetic data is also treated. The estimator was implemented for both the case 1D and 2D, verifying a high linearity and robustness in the estimation. Finally potential application from real world images such SAR images are also discussed.

**Key words:** Estimator, fractal, SAR images

## 1 Introduction

Nowadays, models based on fractality are in almost all the scientific disciplines. Historically, the first fractals were the Cantor set, the Weierstrass function, and the Brownian movement [Coh 13, Fal 90, Pes 02]. These first examples shared some basic concepts that are currently very sought after in many models: self-similarity and certain roughness [Coh 13, Mar 93, Wor 92]. However, to formally define what is a “fractal” or its almost synonymous with “fractional” there are two main axes: the whole object must be similar to each of its parts and its Hausdorff  $\dim_H(\cdot)$  [Fal 90] is not integer. For example, a line  $L$  in the plane has the dimension of Hausdorff  $\dim_H(L) = 1$ , and a set formed by a rectangle with its interior has dimension 2 (it fills all the space in some way). A fractal  $F$  in the  $\mathbb{R}^2$  plane, in contrast, has a dimension  $\dim_H(F)$  in the interval (1,2).

If the exact self-similarity condition is replaced in a probabilistic sense, we get an infinite number of random function graphs (i.e. stochastic processes) that possess the desired property, combined with roughness. The first example and prototype was the Brownian process ( $B_m$ ) [Coh 13, Fal 90]. One of the many problems that arise is that must be chosen a criterion of classification according to its category. According to the probability distribution of the trajectories of this process, this results in a statistical problem of parametric or semi-parametric estimation [Coh13, Mar 93, Wor 92]. A usual parameter for measuring self-similarity is the Hurst parameter  $H$  or similar. For us, a stochastic process will be self-similar if it meets the following definition [Coh 13, Gne

04]. *Definition* : A stochastic process  $X$  is self-similar, with parameter  $H$ , if  $(X(\lambda p))_{p \in \mathbb{R}^n} = (\lambda^H X(p))_{p \in \mathbb{R}^n}$  (where  $\lambda$  is any positive real number and equality is in distribution). In practice the index  $p$  is the time or a spatial coordinate. In some way, the parameter  $H$  governs the roughness of the trajectories as can be seen in the simulations shown in next sections, the greater  $H$  the greater the smoothness of the process realizations.

## 2 Model Synthesis

Patterns were generated according to the model in one dimension (1D) for a discrete interval of points [Cor 1D]. Fig. 1 show the plots for the values obtained considering  $H = 0.3$  and 100, 1000, 10000 and 100000 iteration terms respectively and in all cases for 8192 discrete points. In the aforementioned plots it is observed how the curve becomes more complex as the generated terms increase. Fig. 2 (left) presents a "zoom" for the first 128 points of Fig. 1 (right) ( $H = 0.3$  and 100000 terms), note the similarity in this zoom with Fig. 1 (left), where the 8192 points generated with ( $H = 0.3$ ) are shown but with only 100 terms. In Fig. 2 (center) it is plotted for the case of  $H = 0.9$ . In it you can see a much softer line, with small and soft deviations from a main line. Fig. 2 (right) shows the trajectory achieved for three different  $H$  values:  $H = 0.2, 0.4$  and  $0.8$  for the first, second and third of the 1024 points considered and 100000 terms.

Patterns were generated according to the model in two dimensions (2D) for a discrete interval of points [FracSim]. The 2D data matrix obtained were represented as images files to have a visual perception of the type of fractality generated. They are presented in Fig. 3. Fig. 3 show how the degree of detail increases as the number of terms increases. The matrix generated were 512x512 elements with  $H = 0.3$ . Each element requires the execution of a loop for the desired number of terms. So the whole matrix requires a combination of nested loops and large execution times when large matrix and many terms are considered. For example, the generation of the matrix corresponding to Fig. 3 right requires half an hour of processing on a high-performance PC. Larger matrix with, for example, 1000000 terms, require the use of optimized code and parallel execution to obtain results in reasonable times. Known the value of  $H$  and certain probability distributions it is possible to simulate a wide variety of processes, in the graphics, it is easy to recognize the potentiality to simulate textures in natural images, etc. However, the inverse problem also occurs. Assuming as hypothesis that one or several regions of the image is a realization of one of these processes, then it is of interest to know the parameter  $H$ . An example, that motivated this work in a preliminary way, is a project, carried out by some of the members of the present work, for the automatic identification of oil spills in the sea through the use of satellite images SAR (Synthetic Aperture Radar). Synthetic aperture radar is now commonly used for operational monitoring of oil spills. SAR is the most established for its ability to 'see' through the clouds. Several models, in the same problem, have assumed some kind of local self-similarity in these images [Aiz 01, Ben 99, Guo 09, Pac 19, Ric 14]. In our case, it is reasonable

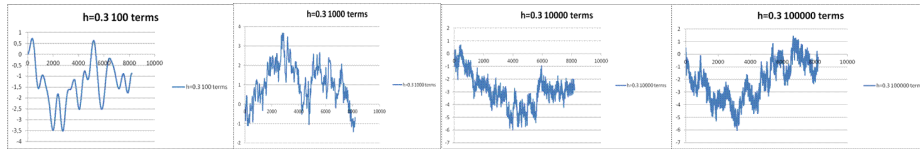


Fig. 1.  $H = 0.3$  with 100, 1000, 10000 and 100000 terms and 8192 discretization points.

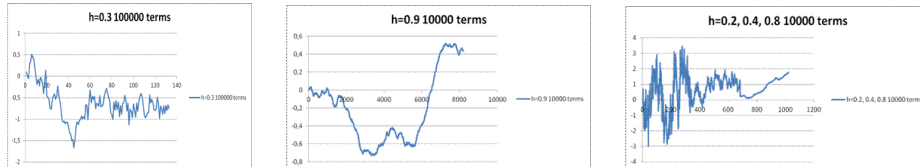
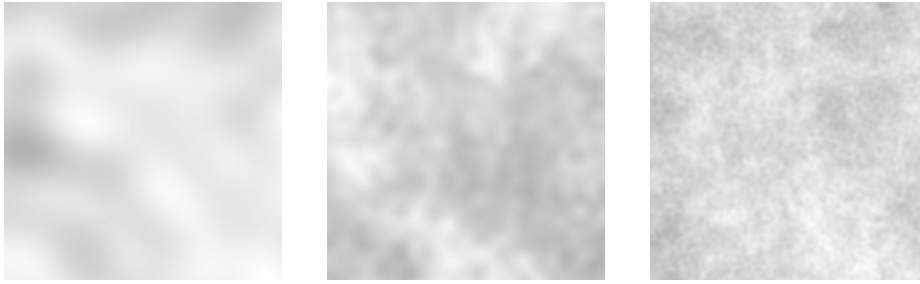


Fig. 2. Left: zoom in the first 128 discret points with  $H = 0.3$ , 100000 terms. Center:  $H = 0.9$ , 10000 terms and 8192 discretization points. Right:  $H = 0.2, 0.4$  y  $0.8$  for the first, second and third of the 1024 points considered and 100000 terms. .

and experimentally verified that the surface of the water in motion, due to the turbulence, presents some kind of self-similarity. In practice this would mean that, for example, the regions without pollution would have a certain value of Hurst,  $H_1$ , on the other hand, the regions contaminated with oil would present a movement with greater damping, which would result in a more soft than the rest, with a value of  $H_2 > H_1$ . These conjectures lead to the problem being solved with a series of hypothesis tests whose central axis is the estimation of the  $H$  parameter.

### 3 Some Experimental Results

In this work we start by estimating  $H$  for case 1D with data generated synthetically for known  $H$ . The estimator was applied to sequences of 8192 data generated for  $H$  values in the range of 0.2 to 0.9. The algorithm applied to each complete sequence of data (the 8192 points) produced estimated values of  $H$  with a strong linear relationship with the real  $H$ . For the same series of data, the application of the estimation of  $H$  in different sub-regions of the series was considered, using continuous data intervals of  $1/2$ ,  $1/4$ ,  $1/8$ , etc., up to very small fractions of the 8192 points. For these estimates of smaller datasets the same  $H$  values were consistently obtained. Patterns were generated according to the model in two dimensions (2D) for a discrete interval of points. The 2D data matrix obtained were represented as images to have a visual perception of the type of fractality generated. They are presented in the figure 3. Figure 3 show how the degree of detail increases as the number of terms increases. The matrix generated were  $512 \times 512$  elements with  $H = 0.3$ . Fig.4 shows the estimation of parameter  $H$  for 2D synthetic images. It was evaluated based on synthetic images with numerous combinations for different values of  $H$ , different amounts



**Fig. 3.**  $H = 0,3$  and  $512 \times 512$  discrete points and from left to right 100 terms, 1000 terms and 10000 terms.

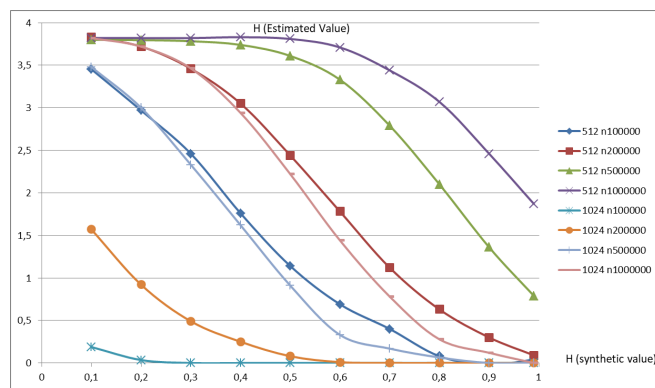


**Fig. 4.** Estimated  $H$  for  $512 \times 512$  and  $1024 \times 1024$  images and addition terms from 100000 to 1000000.

of addition terms and two image resolutions of  $512 \times 512$  points and  $1024 \times 1024$  points. In Fig 4, a linear relationship between the estimated  $H$  and the actual  $H$  can be consistently observed. This allows you to get to the correct estimate easily. It should also be noted that tending towards certain configurations this linearity is lost and different values of  $H$  are no longer distinguishable by estimation. For  $512 \times 512$  images, a greater number of sum terms are leading the curves with a constant saturation towards the lower values of  $H$ . This is because for an image of certain dimensions (small), low  $H$  values make the image more likely to be noise for a greater number of iteration terms. For the  $1024 \times 1024$  images, in a contrasted way, a lower number of sum terms is leading the curves to a constant saturation tending toward zero for the higher values of  $H$ . This is because with few terms and increasing  $H$  values the images become smoother and more similar. With a greater number of terms, the fractality can be developed for increasing values of  $H$  being then possible its detection (linear zone). Once the theoretical and computational models have been validated, finally the application of these techniques to the detection of oil spills in the sea from SAR

images can be overcome. We have started with the analysis of some images, which are anticipated to require some preprocessing to facilitate the task of the estimate sought.

## 4 Conclusions

We presented one and two dimension model synthesis and estimators of self-similarity processes and discussed their possible application to the problem of estimation and detection in real SAR images. In the case of the used 1D estimator, very good results were obtained, with high linearity and robustness in the detection of the Hurst  $H$  parameter. Also very good results were obtained, with high linearity and robustness in the detection of the  $H$  parameter for the 2D case. Some limitations in the estimation for the 2D case also were detected for some configurations involving images resolution, terms of sum and actual  $H$  values of synthesis. This information will be extremely useful when the estimation algorithms will be applied to real SAR images.

## References

- Aiazzi, B., Alparone, L., Baronti, S., Garzelli, A.: Multiresolution Estimation of Fractal Dimension from Noisy Images. *SPIE-IST Journal of Electronic Imaging* 10, 339–348 (2001).
- Benelli, G., Garzelli, A.: Oil-spill Detection in SAR Images by Fractal Dimension Estimation. In: *Proceedings of Geoscience and Remote Sensing Symposium, 1999, IGARSS'99, Hamburg, Germany, 28 June-2 July 1999*, vol. 2, pp. 1123–1126. IEEE Geoscience and Remote Sensing Society, USA (1999)
- Cohen, S., Istas, J.: *Fractional Fields and Applications*. Springer, New York (2013). Cor 1D, <https://github.com/cran/FracSim/find/master>
- Falconer, K.: *Fractal geometry*. John Wiley Sons, New York (1990)
- FracSim. <https://www.jstatsoft.org/article/view/v014i18>
- Gneiting, T., Schlather, M.: Stochastic Models That Separate Fractal Dimension and the Hurst Effect, *SIAM Review*, Vol. 46, No. 2 : pp. 269-282 (2004)
- Guo, W.J., Wang, Y.X., Xie M.X., Cui, Y.J.: Modelling Oil Spill trajectory in coastal waters based on fractional Brownian motion. In: *Marine Pollution Bulletin*, 58, pp. 1339-1346 (2009)
- Maragos, P., Sun, F.K.: Measuring the Fractal Dimension of Signals: Morphological Covers and Iterative Optimization. *IEEE Transactions Signal Processing* 41(1993), 108–121 (1993)
- Pacheco, C., Gambini, J., Delrieux, C.: SAR Image Segmentation based on Multifractal Features, *RPIC2019 XVIII Workshop on Information Processing and Control (RPIC)*, Bahía Blanca, Argentina, 2019.
- Pesquet-Popescu, B., Lévy Véhel, J.: Stochastic Fractal Models for Image Processing: *IEEE Signal Processing Magazine*, IEEE, 19 (5), pp.48-62 (2002)
- Riccio, D., Di Martino, G., Iodice, A., Ruello, G. and Zinno, I.: Fractal dimension images from SAR images, 2014 IEEE International Conference on Image Processing (ICIP), 2014, pp. 106-110, doi: 10.1109/ICIP.2014.7025020.
- Wornell, G.W., Oppenheim, A.: Estimation of fractal signals from noisy measurements using wavelets. *IEEE Transactions Signal Processing* 40, 611–623 (1992)